

# The Design and Analysis of a Runaway Escapement

W. R. Mundy\* en L. Pretorius\*\*  
(First received November 1991, Final version September 1992)

## Abstract

*Runaway escapements of various types are utilised as timing regulators or inertial governors in clockwork mechanisms. The design process for a spring driven runaway escapement having a flat sided pallet has been developed and a computer model to simulate its operation established. Simulation runs were in excellent agreement with experimental results.*

## Nomenclature

$A_j$	motion equation coefficients	$V$	pallet/escape wheel geometry relationship coefficient
$A'$	escape wheel normal contact force moment arm [m]	$\alpha_e$	entrance pallet working surface angle [degree]
$a$	pallet/rotor centre distance [m]	$\alpha_i$	escapement angle [degree]
$c$	entrance pallet radius [m]	$\alpha_x$	exit pallet working surface angle [degree]
$B'$	friction force moment arm on escape wheel [N]	$\theta$	pallet movement angle [degree], (figure 4)
$C'$	friction force moment arm on pallet [N]	$\theta_c$	pallet centre of mass angle [degree], (figure 4)
$D'$	pallet normal contact force moment arm [m]	$\theta_l$	pallet lift angle [degree]
$d$	exit pallet radius [m]	$\dot{\theta}_f$	pallet angular velocity after impact [rad/s]
$e$	coefficient of restitution	$\theta_i$	pallet angular velocity before impact [rad/s]
$F_s$	spring force [N]	$\lambda_e$	angle to entrance pallet [degree]
$F_{xs}, F_{ys}$	spring force components [N]	$\lambda_x$	angle to exit pallet [degree]
$F_{xp}, F_{yp}$	pallet bearing force components [N]	$\mu_1$	friction coefficient (pallet pivot/face)
$i, j$	fixed coordinate system	$\mu_2$	friction coefficient (rotor pivot)
$I_p$	pallet moment of inertia [ $\text{kgm}^2$ ]	$\mu_3$	friction coefficient (rotor bearing)
$I_{pe}$	pallet effective moment of inertia [ $\text{kgm}^2$ ]	$\tau$	escape wheel tooth pitch [degree]
$I_w$	rotor moment of inertia [ $\text{kgm}^2$ ]	$\phi$	escape wheel angle [degree], (figures 5 and 7)
$k$	spring rate [Nm/rad]	$\phi_c$	rotor angle in starting position [degree]
$m_p$	pallet mass [kg]	$\phi_d$	escape wheel drop [degree]
$m_w$	rotor mass [kg]	$\phi_l$	escape wheel starting angle [degree]
$n$	pallet span [no. of teeth]	$\phi_{pt}$	spring pretension [degree]
$\bar{n}_n, \bar{n}_t$	local coordinate system	$\phi_r$	cumulative escape wheel angle [rad]
$P_n$	normal contact force between pallet and rotor [N]	$\dot{\phi}$	rotor angular velocity [rad/s]
$P_v$	rotor gravitational force [N]	$\dot{\phi}_f$	rotor angular velocity after impact [rad/s]
$r_a$	entrance pallet outer circle radius [m]	$\dot{\phi}_i$	rotor angular velocity before impact [rad/s]
$r_{cp}$	pallet centre of mass radius from pivot [m]	$\ddot{\phi}$	rotor angular acceleration [rad s <sup>-2</sup> ]
$r_i$	exit pallet inner circle radius [m]	$\chi_k$	pallet lead [degree]
$r_p$	pallet pivot radius [m]	$\chi_z$	escape wheel tooth tip width [degree]
$r_s$	radius at which spring applies force [m]		
$r_{sp}$	rotor pivot radius [m]		
$r_{s1}$	rotor spring hole radius [m]		
$r_{s2}$	escape wheel dedendum circle radius [m]		
$r_w$	escape wheel addendum circle radius [m]		
$s_4, s_5$	constant positive or negative functions to indicate direction of friction forces, function values -1 or +1		
$S, T$	coincident points on pallet and escape wheel		
$U$	pallet/escape wheel geometry relationship coefficient		

## Introduction

Runaway escapements are utilised as timing regulators or inertial governors in clockwork mechanisms. They are used extensively in the military field as timing regulators in clockwork safety mechanisms and in the toy industry as inertial governors in spring driven toys.

The escapement consists of an escape wheel, which is driven by some energy source, and a pallet which governs the escape wheel angular motion by its interaction with the escape wheel teeth (figure 1).

\* Postgraduate Student, Rand Afrikaans University and Senior Design Engineer, Naschem (Pty) LTD., MSAIMechE

\*\* Professor, Department of Mechanical Engineering, Rand Afrikaans University, MSAIMechE

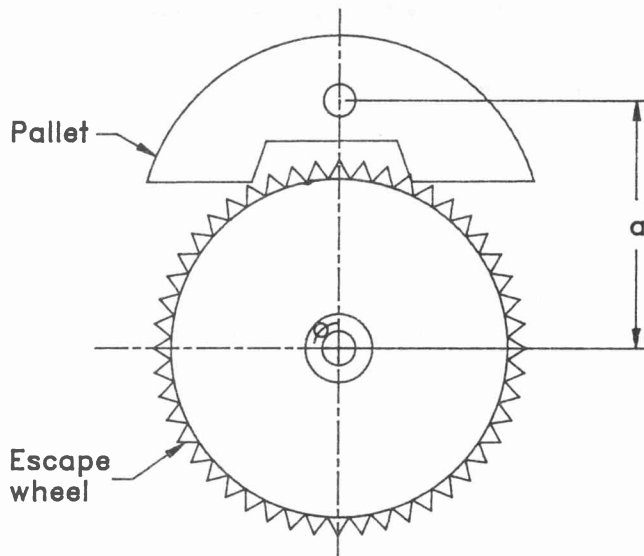


Figure 1: Runaway Escapement with Flat Pallet Faces

This article discusses the geometrical design of escapements having equal armed flat sided pallets then proceeds with the development of a computer model to simulate the motion of this escapement type when it is driven by a helical torsion spring.

The development of a computer model to simulate the motion of a spring driven runaway escapement was undertaken by Mundy [1] to establish a local capability for escapement design. This model was an extension of the work done by Lowen and Tepper [2] which developed a model to simulate the motion of a centrifugal force driven escapement having an unequal armed flat sided pallet.

**Geometrical design theory**

Escapements can be divided into two main categories, namely, those with equal armed pallets and those with unequal armed pallets. The pallets in these two categories can be further divided into those having flat sided pallets and those having pin pallets. This article will cover the geometrical design theory for escapements having equal armed, flat sided pallets.

Equal arm pallets are characterised by the fact that all points on the two lifting surfaces lie between two concentric circles around the centre of motion of the pallet. The geometrical relationships for this type of pallet [3] are shown in figure 2.

In contrast unequal arm pallets are characterized by the fact that the end of lift points on the entrance and exit surfaces both lie on the same circle around the centre of motion of the pallet. The unequal arm pallet is therefore symmetric in appearance about the axis passing between the pallet surfaces and through the centre of motion.

In this article the focus of attention is on the equal arm (asymmetric in appearance) pallet.

If we consider the pallet entrance condition at beginning of lift, see figure 2, the following relationship can be formulated:

$$\alpha_i + \chi_k + \phi_d = n\tau \tag{1}$$

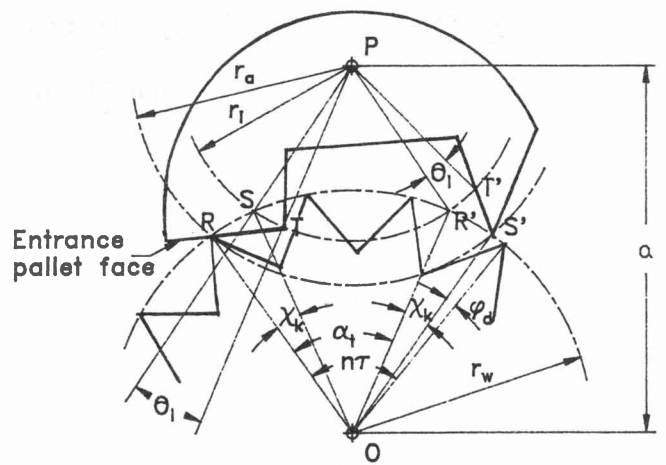


Figure 2: Geometrical Relationships for Equal Arm, Flat sided Pallets

Similarly, considering the pallet exit conditions at beginning of lift, see figure 3, the following relationship may be deduced:

$$\chi_k + \phi_d + (n - 1)\tau = \alpha_i \tag{2}$$

Since the entrance and exit pallet leads are equal, for continuity of motion, the entrance and exit escape wheel drops must be equal. Therefore, from equations 1 and 2 we get

$$\chi_k = \tau/2 - \phi_d \tag{3}$$

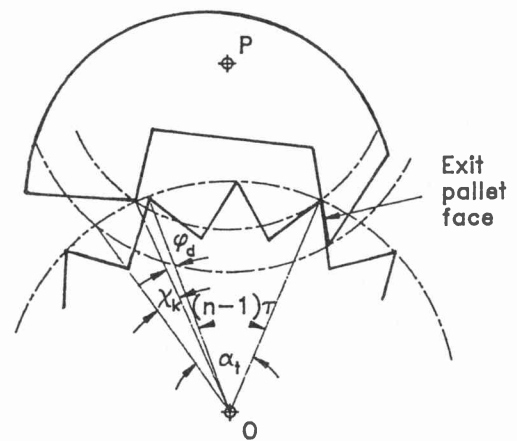


Figure 3: Pallet Exit Condition at Beginning of Lift

If the escape wheel teeth have significant width at their tips,  $\chi_k$  will be reduced by  $\chi_z$  to

$$\chi_k = \tau/2 - \phi_d - \chi_z \tag{4}$$

From equations 1 and 3 we obtain

$$\alpha_i = \tau(n - 1/2) \tag{5}$$

From consideration of figure 2, it can be deduced that

$$r_i = \sqrt{a^2 + r_w^2 - 2r_w a \cos\left(\frac{\alpha_i - \chi_k}{2}\right)} \quad (6)$$

and

$$r_a = \sqrt{a^2 + r_w^2 - 2r_w a \cos\left(\frac{n\tau - \phi_d}{2}\right)} \quad (7)$$

To simplify the design for this type of escapement, the pallet lift angle,  $\theta_i$  can be fixed by choosing point  $T$  on the same straight line as point  $R$  and  $S'$ . The relationship for  $\theta_i$  can again be found by considering figure 2.

$$\theta_i = \arccos\left[\frac{r_i^2 + a^2 - r_w^2}{2ar_i}\right] - \arccos\left[\frac{r_a^2 + a^2 - r_w^2}{2ar_i}\right] \quad (8)$$

The above equations establish the geometrical relationships between the parameters for the equal arm flat sided pallet escapement.

To design an escapement of this type, a few parameters must be chosen to obtain initial design values. These are

1. the escape wheel addendum circle diameter,  $r_w$
2. the number of teeth required on the escape wheel. This determines the pitch,  $\tau$ .
3. the escape wheel flank angle.
4. the escape wheel/pallet centre to centre distance,  $A$ .
5. the escape wheel drop,  $\theta_d$ .
6. the pallet span,  $n$ , and
7. the pallet lift angle,  $\theta_i$  (if a more complex design is required)

The remainder of the design parameter values may then be calculated. To complete the geometrical design, component size, shape and mass properties have to be determined by the designer to suit any constraints which may be imposed, such as space limitations.

**Mathematical analysis**

The mathematical analysis of a spring driven escapement consisting of a spring driven rotor with attached escape wheel and a flat sided equal arm pallet is based on the method of analysis developed by Lowen and Tepper [2]. The major differences are that an equal arm pallet is used (an unequal arm pallet is a simplified version where  $c = d$ ), no gears are used, the rotor/escape wheel is driven by a torsion spring, and disc friction between the rotor and its housing is considered. The analysis also makes allowance for pallets with arbitrarily located centres of mass, friction at the pivots and friction between escape wheel teeth and pallet face.

As in [2], the following three motion regimes are considered:

1. *Coupled motion*, where the escape wheel is in constant contact with one of the pallet surfaces while it is being driven,
2. *Free motion*, where the pallet and escape wheel move independently of each other, and
3. *Impact*, where one of the pallet surfaces is struck by an escape wheel tooth following free motion.

A conservative approach to pivot friction is taken [4] whereby the individual pivot torques are obtained by the algebraic addition of the two friction moments due to the  $x$  and  $y$  components of the normal bearing forces, rather than by the direct use of the resulting normal forces. This assumption was necessary to avoid undue complication in the formulation and solution of the various differential equations. This approach overestimates rather than underestimates the effects of pivot friction.

**Coupled motion equations**

Detailed free body diagrams of the pallet and escape wheel for entrance coupled motion and exit coupled motion are shown in figures 4 to 7. Note that the geometry

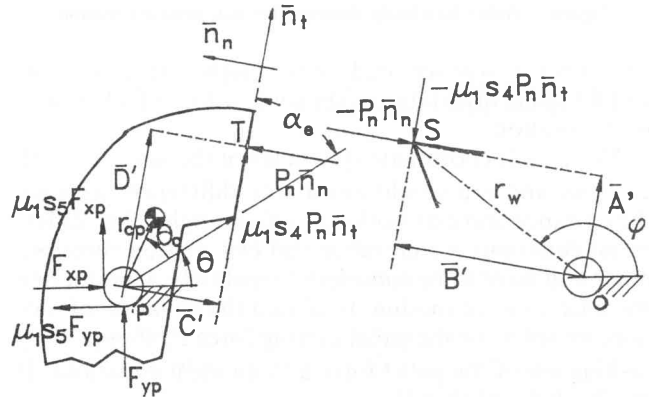


Figure 4: Pallet free body diagram for entrance coupled motion

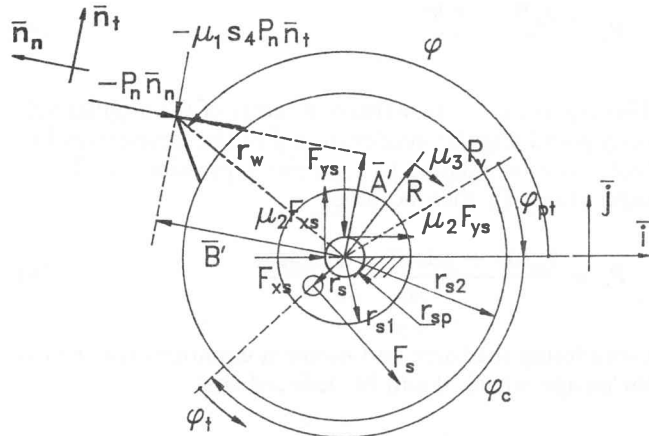


Figure 5: Rotor free body diagram for entrance coupled motion

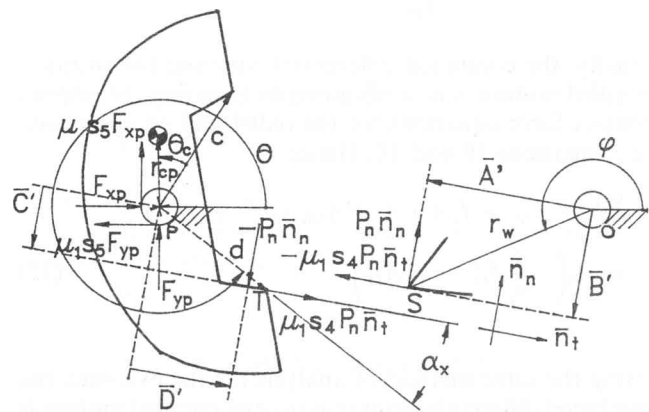


Figure 6: Pallet free body diagram for exit coupled motion

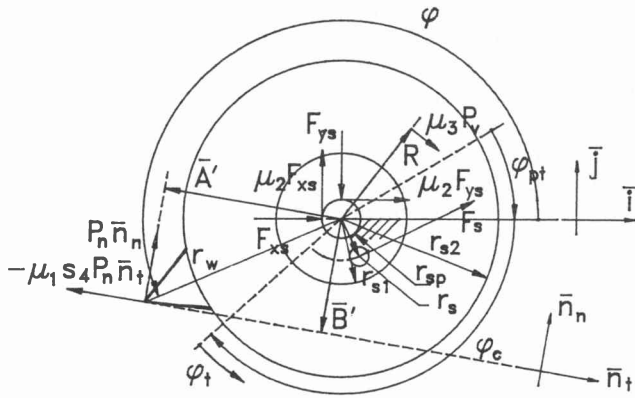


Figure 7: Rotor free body diagram for exit coupled motion

shown here is that required for the mathematical analysis and the pallet orientation is shown here for anti-clockwise rotor rotation.

The  $\bar{n}_t$  -  $\bar{n}_n$  coordinate system is not the same for both entrance and exit conditions due to differences between the entrance and exit working surface angles. The differential equations for entrance and exit motion therefore differ and have to be considered separately. Considering entrance coupled motion, to obtain the equation of motion, we solve for the pallet driving force  $P_n$  (figure 4) by making use of the pallet force and moment equations. It can be deduced that [1]

$$P_n = \frac{I_{pe}\ddot{\theta} - A_8\dot{\theta}^2}{A_7} \quad (9)$$

This equation is now written in terms of the angular velocity  $\dot{\phi}$  and angular acceleration  $\ddot{\phi}$  of the escape wheel so that it can be equated to a similar expression for the escape wheel.  $P_n$  then becomes

$$P_n = \frac{I_{pe}U\ddot{\phi} + (A_8U^2 - I_{pe}V)\dot{\phi}^2}{A_7} \quad (10)$$

Considering the force and moment equations for the rotor/escape wheel, it can be deduced that

$$P_n = \frac{-I_w\ddot{\phi} - \frac{k}{r_s}A_{14} - P_vA_{15}}{A_{16}} \quad (11)$$

Finally, the combined differential equation for entrance coupled motion is now obtained by equating the normal contact force equations for the pallet and escape wheel, i.e., equations 10 and 11. Hence

$$\begin{aligned} & \ddot{\phi}(I_{pe}U A_{16} + I_wA_7) + \dot{\phi}^2 A_{16}(A_8U^2 + I_{pe}V) \\ & = A_7 \left( -\frac{k}{r_s}A_{14} - P_vA_{15} \right) \end{aligned} \quad (12)$$

Using the same method of analysis for the exit side, the combined differential equation for exit coupled motion is obtained as

$$\begin{aligned} & \ddot{\phi}(I_{pe}UA_{22} + I_wA_{19}) + \dot{\phi}^2 A_{22}(A_8U^2 + I_{pe}V) \\ & = A_{19} \left( -\frac{k}{r_s}A_{14} - P_vA_{15} \right) \end{aligned} \quad (13)$$

In the above equations the U and V coefficients are functions only of the geometry of the pallet and escape wheel. The full functional relationships are deduced by Mundy [1].

### Free motion equations

During the free motion phase, the pallet and escape wheel move independently of each other. The escapement motion during this phase will therefore be described by two differential equations; one for the pallet and one for the escape wheel. These differential equations, which are independent of entrance or exit motion, are obtained by setting the normal force equations for the pallet (equation 9) and escape wheel (equation 11) equal to zero. The pallet free motion differential equation becomes

$$I_{pe}\ddot{\theta} + A_8\dot{\theta}^2 = 0 \quad (14)$$

and the escape wheel free motion differential equation becomes

$$I_w\ddot{\phi} = -\frac{k}{r_s}A_{14} - P_vA_{15} \quad (15)$$

### Impact equations

The impact analysis is based on the classical angular impulse-momentum model, where a coefficient of restitution is used to account for the energy losses.

The following assumptions are made:

1. The angular impulse on the escape wheel due to its torque is small in comparison to the impact force between pallet and escape wheel [5][2][6].
2. The tangential impulsive force due to friction,  $\mu_1 P_n$ , is small in comparison to the normal impulsive force,  $P_n$  [5][2].

It is therefore assumed that the only impulsive forces which act on the pallet and escape wheel are the mutual normal impulsive force  $P_n$  and the impulsive reactions at the pivots.

In general [6], we have that

*System momenta at time  $t_1$  + System external impulses applied from time  $t_1$  to time  $t_2$  = System momenta at time  $t_2$*

and

$$e = \frac{\text{relative velocity after impact}}{\text{relative velocity before impact}}$$

Using suitable expressions for above two terms, it can be deduced that [1]

$$\dot{\theta}_f = \frac{e(\dot{\phi}_i A' - \dot{\theta}_i D') + \dot{\phi}_p A'}{D'} \quad (16)$$

and

$$\dot{\phi}_f = \frac{\dot{\theta}_i I_p D' A' (1 + e) + \dot{\phi}_i (I_w D'^2 - I_p A'^2 e)}{I_w D'^2 + I_p A'^2} \quad (17)$$

With the equations of motion for a spring driven runaway escapement with a flat sided pallet now available, a computer simulation model of this escapement can now be developed.

**Computer model**

The computer model of the spring driven escapement was based on the same principles as those developed by Lowen and Tepper [5][2], however in this case, Advanced Continuous Simulation Language (ACSL) was used as opposed to formal Fortran. This was done to simplify the solving of the system differential equations as well as to make the model more versatile.

The simulation model of the escapement was assumed to begin halfway through entrance coupled motion [2] at an initial escape wheel angle  $\phi$  of  $\phi_1$  degrees. This corresponds to an escape wheel starting angle,  $\phi_c$ , and a cumulative escape wheel angle,  $\phi_i$ , of  $0^\circ$ . See figure 8. This starting angle is taken to be the angle through which the rotor must move from beginning to end of motion.

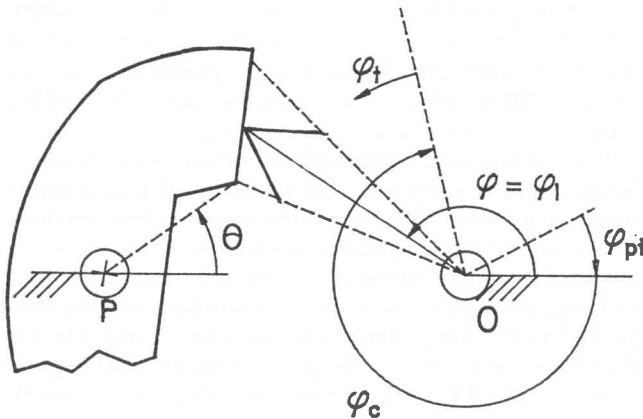


Figure 8: Escapement Starting Position

The model begins with the reading in of the input data then starts with the solving of the entrance coupled motion equations. A fourth order Runge-Kutta integration routine within ACSL is used to solve the coupled and free motion differential equations. A flow diagram of the computer model developed by Mundy [1] is shown in figure 9.

An indexing operation is performed on  $\theta$ ,  $\theta_c$  and  $\phi$  to provide initial conditions as control transfers from the entrance to exit sides and vice versa as the pallet oscillates. The escape wheel angle,  $\phi$ , therefore varies continuously between the entrance and exit sides. The cumulative escape wheel angle,  $\phi_i$ , is therefore measured by continuously adding the angular increments,  $\Delta\phi$ , due to each cycle of integration.

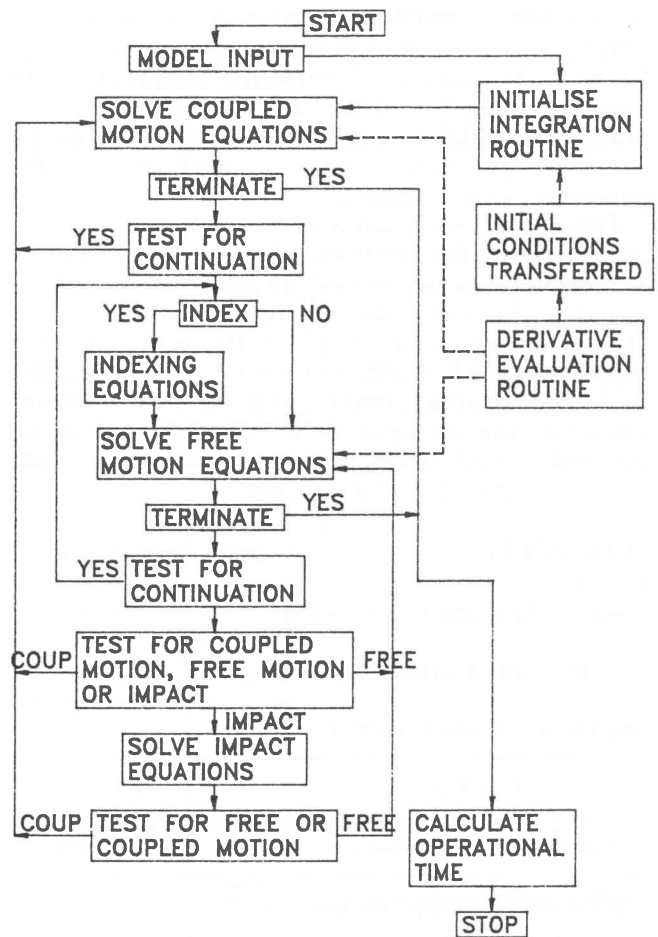


Figure 9: Flow diagram of escapement model

A test angle is used to determine whether entrance or exit motion is to be evaluated, and contact sensing parameters are used to determine motion status. The techniques used to determine the status of each motion regime during escapement operation so that control may be passed to the applicable equations of motion are discussed fully by Mundy [1].

The simulation finally terminates when either  $\phi_i = |\phi_c|$  which corresponds to the end of rotor motion or when the escapement operating time exceeds or is equal to a desired stop time. This last condition ensures that the program will stop in the event of model parameters being chosen such that the model slows down drastically before the desired rotor rotation is reached.

This computer model was now tested for accuracy.

**Practical escapement parameters**

To provide practical escapement parameters and a means of testing the computer simulation program, two escapements were designed. A single rotor was designed for both escapements.

The escapements were designed using engineering judgement and the equations developed from the geometric principles. The pallets were designed to be as symmetrical as possible for ease of manufacture. To this end, the special case where the entrance pallet face and the end of the exit pallet face lay on the same straight line was

chosen. This enabled the pallet lift angle,  $\phi_l$  to be calculated from equation 8. Mass properties of the rotor and pallets were obtained after the respective components were modelled using the 3-D solid modelling package by SDRC called I-DEAS 4.0. The list of applicable escape wheel/rotor parameters is given in table 1 and the pallet parameters given in table 2.

The arming time of each escapement variation was tested by recording the vibrations induced by the escapement as it operated. In this method, an accelerometer was attached to the base of the test rig and connected to an oscilloscope via a charge amplifier. The oscilloscope was triggered by the first impact of a rotor tooth on a pallet face. The rotor arming time was then that time which was measured from the trigger pulse to when a final impact occurred between a rotor tooth and a pallet face, or when the rotor impacted with a stop pin.

PARAMETERS	VALUE
escape wheel addendum radius, $r_w$	11,0 mm
escape wheel dedendum radius, $r_{s2}$	9,5 mm
escape wheel tooth pitch, $\tau$	7,5°
rotor pivot radius, $r_{sp}$	1,0 mm
rotor spring hole radius, $r_{s1}$	2,0 mm
radius where spring applies force, $r_s$	1,5 mm
rotor mass, $m_w$	23,12 g
rotor moment of inertia, $I_w$	1,190 kgmm <sup>2</sup>

**Table 1:** Parameters for Rotor Design

PARAMETERS	PALLET 1	PALLET 2
pallet/rotor centre distance, $a$	15,5 mm	14,5 mm
escape wheel drop, $\phi_d$	1,0°	1,0°
pallet span, $n$	8	8
pallet lead, $\chi_k$	2,75°	2,75°
escapement angle, $\alpha_i$	56,25°	56,25°
pallet lift angle, $\theta_l$	2,97°	2,95°
pallet outer radius, $r_a$	8,03 mm	7,33 mm
pallet inner radius, $r_i$	7,54 mm	6,81 mm
pallet pivot radius, $r_p$	1,0 mm	1,0 mm
pallet mass, $m_p$	14,4 g	12,1 g
pallet moment of inertia, $I_p$	0,669 kgmm <sup>2</sup>	0,508 kgmm <sup>2</sup>
pallet centre of mass radius, $r_{cp}$	1,50 mm	0,92 mm
pallet centre of mass angle, $\theta_c$	-38,67°	-44,63°

**Table 2:** Parameters for Equal Arm Pallets

Due to the time lag between rotor release and first impact, this method was expected to give an error of  $\pm 2\%$ .

## Results

The accuracy of this simulation model was checked by using the geometrical parameters, mass properties, and spring data of each tested escapement as input.

General parameters affecting motion, which are the coefficients of friction and restitution, were chosen. The coefficients of kinetic friction for brass on brass and steel on brass were both assumed to be 0,3. High speed motion pictures of escapement operation [2] showed that escape wheel tooth/pallet impacts were essentially inelastic. The coefficient of restitution was therefore assumed to be equal to zero.

The practical and simulated test results are shown in table 3. For the purpose of calculating errors between theoretical and practical operating times, the minimum time measured practically was used since this time is always the most significant.

	operational time (ms)		error (%)
	as tested	simulated	
escapement 1	718	712	0,8
escapement 2	690	673	2,5

**Table 3:** Escapement operating time test results

Strip plots generated from the computer run of escapement 2 showing the angular motion of the rotor,  $\phi_t$  (PHT),  $\dot{\phi}$ (PHD) and  $\ddot{\phi}$ (PHDD), are shown in figure 10. The first 100 ms of rotor motion are shown in figure 11 to illustrate the movement more clearly.

From these figures, it can clearly be seen how the angular position, velocity and acceleration of the escapement rotor varies with time during the three motion regimes. For example, the angular acceleration of the rotor increases during exit coupled motion and decreases during entrance coupled motion. This shows that entrance coupled motion is the prime contributing factor in governing the escapement motion. The plots of escapement angular motion could therefore be used as tools to access the effectiveness of escapement designs.

## Conclusions

A reasonably accurate computer simulation model of a spring driven escapement having flat sided pallet with either equal or unequal arms has been successfully developed. Simulation runs gave excellent results when compared to actual test results (operating time error < 3%).

The computer model is particularly suited to parametric studies. The effects of factors such as coefficient of restitution, coefficient of friction, component mass and moment of inertia, component dimensions and spring rate on escapement operational time may be easily determined. Of particular importance is the fact that the effects of changes in component dimensions on escapement operational time may be determined. This allows components to be correctly dimensioned on manufacturing drawings.

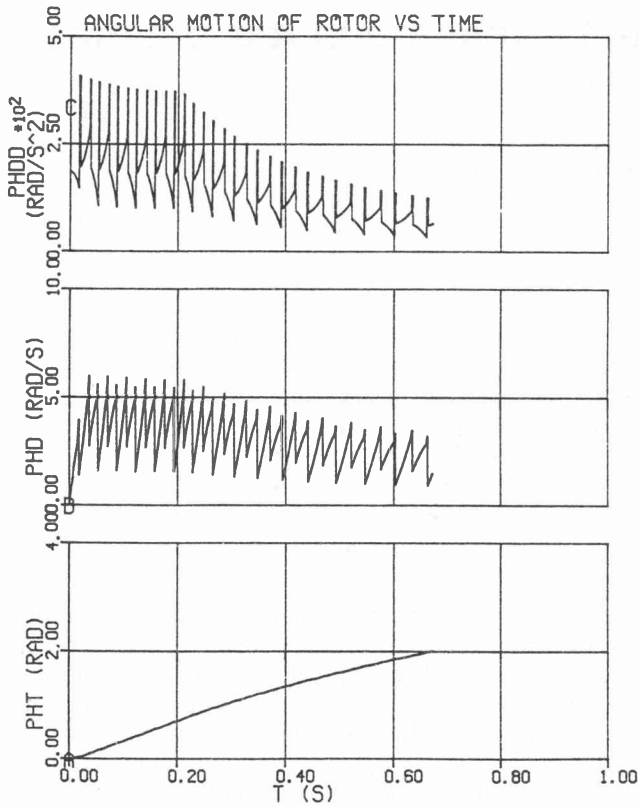


Figure 10: Strip plots of rotor angular motion for escapement 2

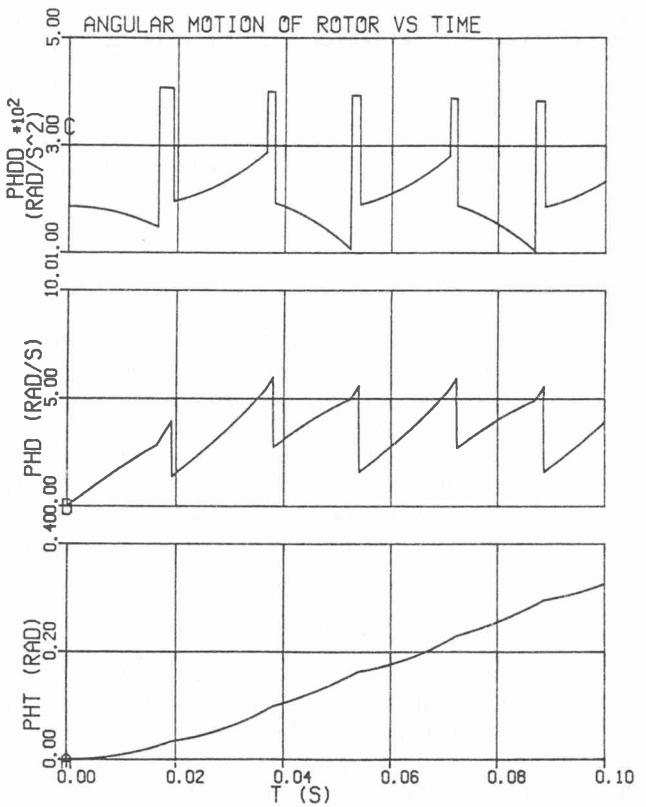


Figure 11: Initial angular motion plots of escapement 2

It follows then that the model allows this escapement type to be fully designed and modelled on paper. This ensures that development time and cost is kept to a minimum and that escapements can be built as cheaply as possible and yet still provide the desired operational times.

**References**

1. Mundy, W. R., "The Analysis of Runaway Escapements Utilised in Clock-work Mechanisms", M Eng Thesis, September 1991, Rand Afrikaans University.

2. Lowen, G. G., and Tepper, F. R., "Computer Simulation of Artillery S & A Mechanism (involute gear train and straight-sided verge runaway escapement)"; Technical Report ARLCD-TR-82013, ARRADCOM, Dover, NJ. November 1982.  
 3. Assmus, F. R., "Fundamentals Concerning Technical Mechanisms", Springer Verlag, p 168 (translated), Berlin. 1958.  
 4. Lowen, G. G., and Tepper, F. R., "Fuze Gear Train Analysis", Technical Report ARLCD-TR-79030, ARRADCOM, Dover, NJ. December 1979.  
 5. Lowen, G. G., and Tepper, F. R., "Dynamics of the Pin Pallet Runaway Escapement", Technical Report ARLCD-TR-77062, ARRADCOM, Dover, NJ. June 1978.  
 6. Beer, F. P., and Johnston, E. R., "Vector Mechanics for Engineers: STATICS & DYNAMICS", McGraw-Hill, New York, 1972.